Hindawi
Mathematical Problems in Engineering
Volume 2019, Article ID 5932742, 9 pages
https://doi.org/10.1155/2019/5932742

Research Article

Short-Crested Wave-Current Forces on Composite Bucket Foundation for an Offshore Wind Turbine

Piguang Wang[1,2] **Mi Zhao**[1] **and Xiuli Du**[1]

[1]*Beijing University of Technology, Beijing 100124, China*
[2]*Tsinghua University, Beijing 100084, China*

Correspondence should be addressed to Mi Zhao; zhaomi@bjut.edu.cn

Received 20 June 2018; Revised 10 November 2018; Accepted 9 January 2019; Published 29 January 2019

Academic Editor: Maurizio Brocchini

An analytical solution for the diffraction of short-crested incident wave with uniform current on a composite bucket foundation is derived. The influences of the uniform current on wave frequency, wave run-up, wave force, and inertia and drag coefficients on the composite bucket foundation are investigated. The numerical results indicate that the current incident angle and current velocity have significant effects on the short-crested wave run-up, wave force, and inertia and drag coefficients on the composite bucket foundation. For a fixed wave number, the wave frequency, wave run-up, wave forces, and inertia and drag coefficients obviously increase with the increase of current velocity when the relative angle between the current velocity and wave propagation direction is smaller than 90°, whereas they obviously decrease when the relative angle is larger than 90°. It also can be found that the effect of wave-current interaction on the short-crested wave increases with the increase of the total wave number and the decrease of the water depth. The short-crested wave forces will be significantly increased when the current incident angle parallels to the direction of the wave propagating. Therefore, the short-crested wave-current load should be carefully considered in the design of the composite bucket foundation for an offshore wind turbine.

1. Introduction

Offshore wind power is one of the most important renewable green resources in the world. The interest in exploitation of wind energy offshore has been growing, as reported in [1, 2]. Monopole, tripod, jacket structures, gravity-base, and suction caisson foundations have been widely used in the development of offshore wind powers [3]. Many experimental and numerical studies have been conducted on offshore wind turbines, such as the monopile [4], jacket support structure [5], tripod [6], and floating offshore wind turbines [7]. In recent years, a large number of offshore windfarms have already been installed, are under construction, or are being planned in China [8], and a new kind of suction foundation called composite bucket foundation for offshore wind turbines was proposed by Tianjin University [9–12]. The composite bucket foundation takes full advantage of the high tensile capacity of the steel strand and the high compressive capacity of the concrete. Compared to conventional foundations, it has the advantages of reducing construction costs and shorting construction time.

Wave forces on offshore structures are one of the dominated form loads generally encountered in ocean environment. To safely design the offshore wind turbines, it is critical to appropriately evaluate the wave loads on the composite bucket foundation. However, the wave forces on the composite bucket foundation are not well studied. Wave forces on slender bodies are generally estimated by the formula proposed by Morison et al. [13]. It is assumed that the presence of the object has no effects on the characteristics of the incident wave field in the Morison equation. The Morison equation does not account for breaking waves, but it is still applied in practice. However, the determination of wave forces on large-scale offshore structures is quite complex because of the scattered waves in the vicinity of the offshore structure.

The diffraction theory can be employed to compute the wave forces on large-scale structures. MacCamy and Fuchs [14] proposed a closed form solution to estimate the wave forces on a large vertical circular cylinder subjected to linear plane waves being diffracted around a large vertical circular

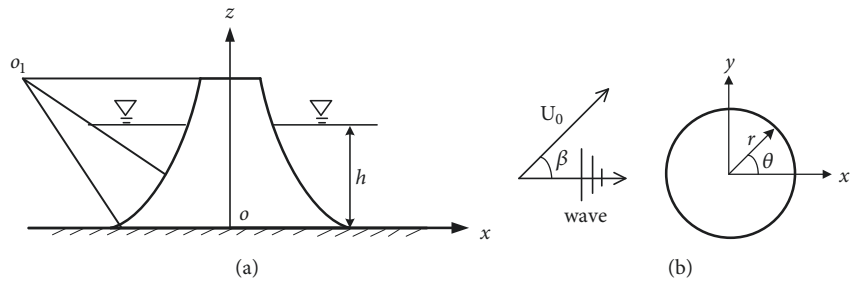

Figure 1: Definitions of arc transition of composite bucket foundation: (a) side view and (b) top view.

cylinder. The analytical results have been proved by experiments [15, 16] and numerical models [17, 18]. Thereafter, the diffraction theory is generally used to solve the problems for linear plane waves being diffracted around large-scale structures [19–25]. However, most waves generated by wind blowing the water surface in oceans are much better modeled by short-crested waves than by plane waves. Short-crested waves are doubly periodic in two horizontal directions, one in the direction of propagation and the other normal to it [26]. Recently, the problems about short-crested wave diffraction around large-scale structures are investigated by many researchers [27–29].

In fact, ocean current is also an important load in real oceans, whose presence may drastically alter the wave conditions. The coexistence of waves and currents is a common feature of most ocean environments. It is well known that the effects of wave-current interaction are more dramatic for strong currents. However, it is also found that even a relatively weak current of the open ocean exerts an appreciable and may change the wavelength, amplitude, direction of propagation and energy density spectrum of gravity waves. Tung and Huang [30] investigated the effect of wave-current interaction on the wave force exerted on slender cylindrical elements by the Morison equation. Based on the diffraction theory approach, Watanabe [31] investigated the effect of plane wave-current interaction on the wave force exerted on large structures, and Jian et al. [32] investigated the effect of short-crested wave-current interaction on the wave force exerted on large circular cylinders.

In literature there are very few studies on the wave forces on a composite bucket foundation by using analytical, experimental, or numerical method. Lian et al. [33] derived the analytical solution for calculating the linear plane wave force on a composite bucket foundation. Furtherly, Wang et al. [34] derived the analytical solution for calculating the wave force on a composite bucket foundation subjected to short-crested waves. The research conducted by Jian et al. [32] indicated that the total wave forces exerted on a cylinder with currents would be larger compared to the wave forces exerted by pure short-crested waves. This study is mainly to investigate the short-crested wave-current forces around a composite bucket foundation with uniform current. An analytical solution for the diffraction of short-crested incident wave on axisymmetric structures with uniform current is derived. The results will provide a useful guide for the design of offshore wind turbines.

2. Formulation of the Problem

The model of the composite bucket foundation given by Lian et al. [33] is investigated in this study as shown in Figure 1. The composite bucket foundation is a kind of fixed axisymmetric structure, which is assumed to be rigid and placed on the floor of the ocean with uniform depth, h. As shown in Figure 1, the Cartesian coordinate system O-xyz and the cylindrical coordinate system O-$r\theta z$ are defined, where O and O_1 are the origin of the Cartesian coordinate system and the circle center of the arc transition and z-axis points upwards from the seabed, respectively. The arc transition equation of the surface of composite bucket foundation in cylindrical coordinate system is expressed as $r = 20.44 - \sqrt{121.19 - z^2 + 28.2z}$.

The following notations are used in the paper: t is the time variable; h is the water depth and it is 8m in the study; g is the gravitational acceleration; k is the total wave number; H is the wave height; ρ is the water density; ω is wave frequency; a is the radius of the composite bucket foundation at z; $\phi = \phi_I + \phi_S$ is the total velocity potential function; $\phi_I(r, \theta, z, t)$ is the incident wave velocity potential; and $\phi_S(r, \theta, z, t)$ is the scattered velocity potential. The fluid is assumed incompressible, inviscid, and irrotational. It is assumed that the short-crested wave propagates along the positive x-axis with a steady uniform current U_0 at an angle β to the direction of the incident wave.

For short-crested incident waves traveling in the positive x-direction with uniform current, the velocity potential can be expressed as the real part of [32, 35]

$$\phi_I = -\mathrm{i}\frac{gH}{2\omega^*}\frac{\cosh kz}{\cosh kh}\mathrm{e}^{\mathrm{i}(k_x x - \omega t)}\cos\left(k_y y\right) \tag{1}$$

in which ω^* is the incident wave angular frequency of still water relative to a frame of reference moving with the current U_0, $k = \sqrt{k_x^2 + k_y^2}$ is the total wave number, and k_x and k_y are the wave numbers in the x-direction and y-direction.

The dispersion relation for short-crested waves on uniform current can be derived as

$$\left(\omega - \vec{k}.\vec{U}_0\right)^2 = \left(\omega^*\right)^2 = gk\tanh kh \tag{2}$$

in which $\vec{k} = (k_x, k_y)$; $\vec{U}_0 = |\vec{U}_0|(\cos\beta, \sin\beta)$ denote the uniform current components in x-axis and y-axis directions respectively; $\omega^* = \omega - \vec{k}.\vec{U}_0 = \omega - k|\vec{U}_0|\cos(\alpha - \beta)$ is the

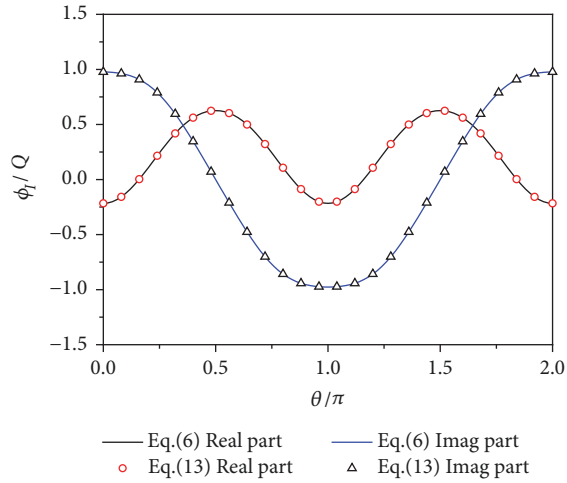

FIGURE 2: Comparison of (6) and (13) with kr=2, k_x/k=0.5 and r=1m.

relative angular frequency; and $\alpha = \arccos(k_x/k)$ denotes the wave propagation direction.

In cylindrical coordinate system, the incident wave velocity potential given in (1) can be rewritten as

$$\phi_I = -\mathrm{i}\frac{gH}{2\omega^*}\frac{\cosh kz}{\cosh kh}\mathrm{e}^{-\mathrm{i}\omega t}\sum_{n=0}^{\infty}\varepsilon_n J_n(kr)\cos n\theta\cos n\alpha \tag{3}$$

where $\varepsilon_0 = 1$ and $\varepsilon_n = 2\mathrm{i}^n$ for $n \geq 1$ and J_n is the Bessel function of the first kind of order n. Figure 2 shows the comparison of (1) and (3) with kr=2, k_x/k=0.5, and r=1m, where $Q = -\mathrm{i}(gH/2\omega^*)(\cosh kz/\cosh kh)\mathrm{e}^{-\mathrm{i}\omega t}$. It can be seen that (3) is in full accord with (1).

The governing equation and boundary conditions for the scattered wave can be expressed as

$$\frac{\partial^2\phi_S}{\partial r^2} + \frac{1}{r}\frac{\partial\phi_S}{\partial r} + \frac{1}{r^2}\frac{\partial^2\phi_S}{\partial\theta^2} + \frac{\partial^2\phi_S}{\partial z^2} = 0 \tag{4}$$

$$\left(\frac{\partial}{\partial t} + \vec{U}_0\nabla\right)^2\phi_S + g\frac{\partial\phi_S}{\partial z} = 0 \quad z = h \tag{5}$$

$$\frac{\partial\phi_S}{\partial z} = 0 \quad z = 0 \tag{6}$$

$$\frac{\partial\phi_S}{\partial \boldsymbol{n}} = -\frac{\partial\phi_I}{\partial \boldsymbol{n}} \quad r = a \tag{7}$$

where $\boldsymbol{n}$ denotes the normal of the foundation. The scattered wave ϕ_S also should satisfy the radiation condition at infinity.

3. The Analytical Solution of the Problem

The solution for the scattered wave is expressed by satisfying (4)-(7) as

$$\phi_S = -\mathrm{i}\frac{gH}{2\omega^*}\frac{\cosh kz}{\cosh kh}e^{-\mathrm{i}\omega t}\sum_{n=0}^{\infty}A_n H_n^{(1)}(kr)\cos n\theta \tag{8}$$

in which A_n are undetermined coefficients, $H_n^{(1)}$ is the Hankel function of the first kind of order n, and the prime denotes a derivative with respect to the argument.

Thus, the total velocity potential in the wave field can be expressed as follows.

$$\phi = -\mathrm{i}\frac{gH}{2\omega^*}\frac{\cosh kz}{\cosh kh} \cdot e^{-\mathrm{i}\omega t}\sum_{n=0}^{\infty}\left[\varepsilon_n J_n(kr)\cos n\alpha + A_n H_n^{(1)}(kr)\right]\cos n\theta \tag{9}$$

Substituting (9) into (7), coefficients A_n can be rendered as

$$A_n = -\varepsilon_n\cos n\alpha\frac{\tanh kzJ_n(ka) + \mu J_n'(ka)}{\tanh kzH_n^{(1)}(ka) + \mu H_n^{(1)\prime}(ka)} \tag{10}$$

where $\mu = \partial z/\partial r$.

Applying the total velocity potential (9), the free surface wave elevation on the surface of the composite bucket foundation can be obtained as follows.

$$\eta = -\frac{1}{g}\frac{\partial\phi}{\partial t}\bigg|_{z=h} = \frac{H\omega}{2\omega^*}e^{-\mathrm{i}\omega t}\sum_{n=0}^{\infty}S_n\varepsilon_n\cos n\alpha\cos n\theta \tag{11}$$

$$S_n = J_n(ka) - \frac{\tanh kzJ_n(ka) + \mu J_n'(ka)}{\tanh kzH_n^{(1)}(ka) + \mu H_n^{(1)\prime}(ka)}H_n^{(1)}(ka) \tag{12}$$

The pressure at any point on the surface of the composite bucket foundation can be calculated from the linearized Bernoulli equation.

$$p(a,\theta,z) = -\rho\frac{\partial\phi}{\partial t} = \frac{\rho gH\omega}{2\omega^*}\frac{\cosh kz}{\cosh kh}e^{-\mathrm{i}\omega t}\sum_{n=0}^{\infty}S_n\varepsilon_n\cos n\alpha\cos n\theta \tag{13}$$

The force component per unit length in the direction of the positive x-axis can be expressed as follows.

$$\frac{\mathrm{d}F_x}{\mathrm{d}z} = -\pi a\rho gH\frac{\omega}{\omega^*}\frac{\cosh kz}{\cosh kh}\cos\alpha\cos\alpha_0 S_1\mathrm{i}e^{-\mathrm{i}\omega t} \tag{14}$$

The total horizontal force on the composite bucket foundation, F_x, computed by integrating the expression of (14) with respect to z, can be obtained as follows.

$$F_x = \int_0^h\frac{\mathrm{d}F_x}{\mathrm{d}z}\mathrm{d}z = -\frac{\pi\rho gH}{\cosh kh}\frac{\omega}{\omega^*}\cos\alpha\mathrm{i}e^{-\mathrm{i}\omega t}\int_0^h a\cosh kz\cos\alpha_0 S_1\mathrm{d}z \tag{15}$$

For slender cylinders, inertia and drag coefficients have been investigated, for example, for the occurrence of large waves in a 3D field interacting with a current in [36]. In general, the Morison force is considered, with velocity and acceleration in the undisturbed field, and the force related to the drag and inertia coefficient. Drag and inertia coefficient for the Morison force are calculated from experimental

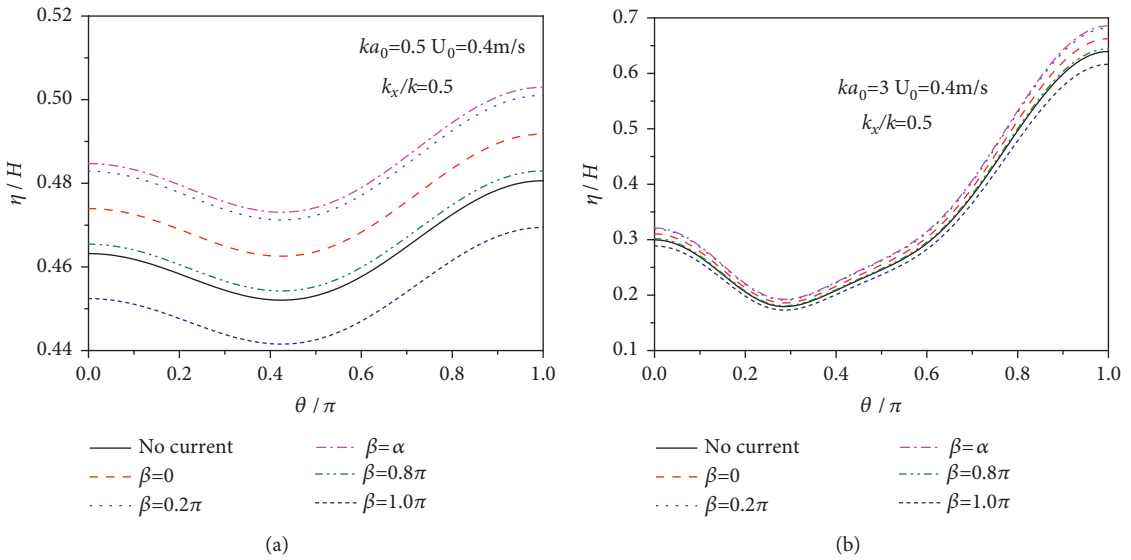

FIGURE 3: Wave run-up on the composite bucket foundation for different current incident angle: (a) ka_0=0.5 and (b) ka_0=3.

activity usually. For example, the inertia and drag coefficients have been achieved with a field experiment at sea in [37], for random 3D waves acting on a cylinder. For larger cylinders, the approach in which the force takes into account the drag and the inertia contributions proposed by Mei [38] is adopted in the present study, where the component of force per unit of wave height in phase with the particle acceleration of the incident waves is called an effective inertia coefficient and that in phase with the particle velocity is termed an effective linear drag coefficient.

Following Mei [38], the inertia coefficient C_M and drag coefficient C_D per unit height for the short-crested waves with current will be introduced, which are related to the added mass and damping coefficients in the restoring forces on a structure in forced radiation. For the composite bucket foundation, the inertia and drag coefficients per unit height are related to the total force per unit length as

$$\mathrm{Re}\left(\frac{\mathrm{d}F_x}{\mathrm{d}z}\right) = \rho\pi a_0^2\left(\frac{C_M\partial U}{\partial t} + \omega C_D U\right) \tag{16}$$

where U means the velocity of the incident short-crested wave at $x = 0$ in the absence of the composite bucket foundation. Following Zhu [26], without the constant term $0.5\rho gH\cosh kz/\cosh kh e^{-\mathrm{i}\omega t}$, the total force per unit length can be expressed as follows.

$$\frac{\mathrm{d}F_x/\mathrm{d}z}{\left[0.5\rho gH\cosh kz/\cosh kh e^{-\mathrm{i}\omega t}\right]} = \pi a_0^2 k_x\sqrt{C_M^2 + C_D^2} \tag{17}$$

Thus, the inertia coefficient C_M and drag coefficient C_D are defined as

$$C_M = -\frac{\mathrm{Im}\left\{(\mathrm{d}F_x/\mathrm{d}z)/\left[0.5\rho gH(\cosh kz/\cosh kh)e^{-\mathrm{i}\omega t}\right]\right\}}{(\pi a_0^2 k_x)} \tag{18a}$$

$$C_D = \frac{\mathrm{Re}\left\{(\mathrm{d}F_x/\mathrm{d}z)/\left[0.5\rho gH(\cosh kz/\cosh kh)e^{-\mathrm{i}\omega t}\right]\right\}}{(\pi a_0^2 k_x)} \tag{18b}$$

where Im and Re denote imaginary and real parts. After some simplification, the inertia coefficient C_M and drag coefficient C_D can be expressed as follows.

$$C_M = \frac{2\omega a}{\omega^* k_x a_0^2}\mathrm{Im}\left\{\mathrm{i}S_1\cos\alpha\cos\alpha_0\right\} \tag{19a}$$

$$C_D = -\frac{2\omega a}{\omega^* k_x a_0^2}\mathrm{Re}\left\{\mathrm{i}S_1\cos\alpha\cos\alpha_0\right\} \tag{19b}$$

4. Results and Discussion

A series of numerical examples at a fixed time are carried out to investigate the effects of current on the wave run-up of short-crested wave on the composite bucket foundation. Figure 3 shows the dimensional wave run-up η/H on the composite bucket foundation against variable θ/π for different current incident angle β and ka_0 with k_x/k=0.5 and U_0= 4m/s, where a_0 denotes the radius of the composite bucket foundation at z=0. It can be seen that the wave run-up on the composite bucket foundation is quite different when the value of ka_0 is changed and it is significantly changed by the current. Figure 4 shows the dimensional run-up η/H at $\theta = \pi$ on the composite bucket foundation against variable $|\alpha - \beta|$ for different current velocity U_0 and k_x/k with ka_0=1, where $|\cdot|$ denotes the absolute value and $|\alpha - \beta|$ is the relative angle between the current velocity and wave propagation direction. Figure 5 shows the wave frequency against variable $|\alpha - \beta|$ for different current velocity U_0 and k_x/k with ka_0=1. It can be seen from Figure 4 that the current velocity has significant influence on the wave run-up on the composite bucket foundation and it sharply decreases as $|\alpha-\beta|$ increases.

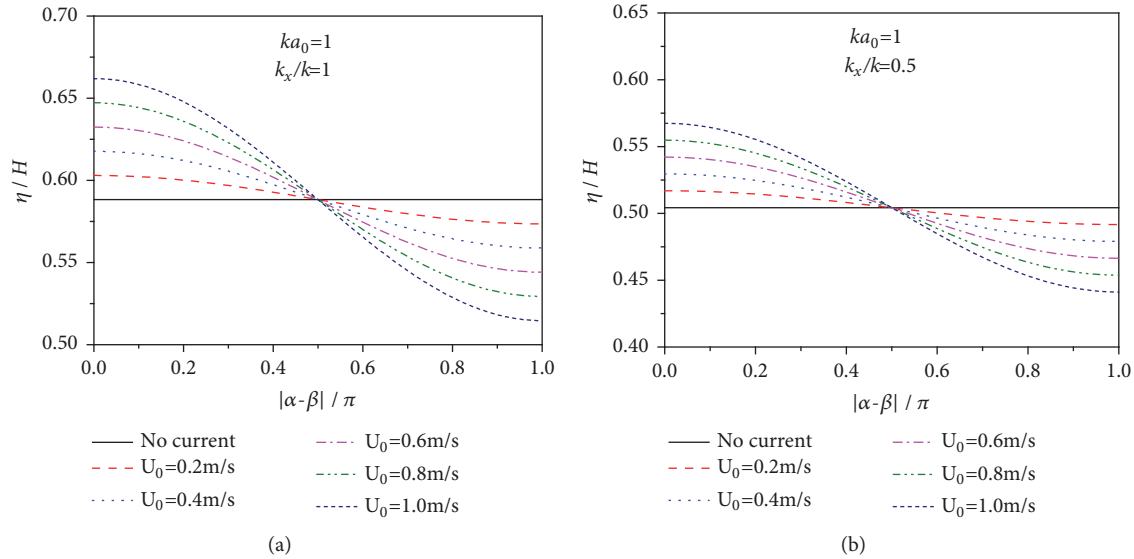

FIGURE 4: Wave run-up versus $|\alpha - \beta|$ at $\theta=\pi$ on the composite bucket foundation for different current velocity: (a) k_x/k =1 and (b) k_x/k =0.5.

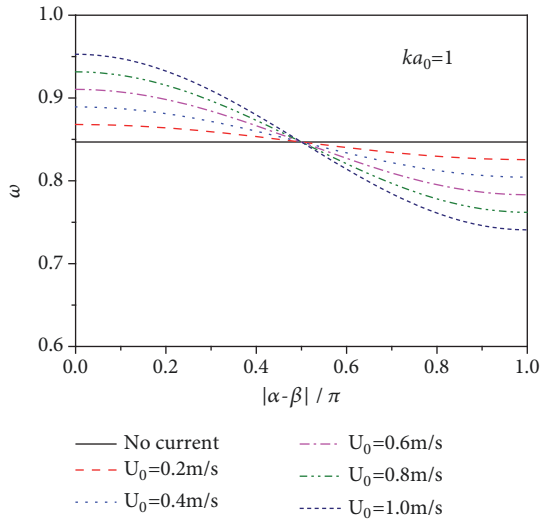

FIGURE 5: Wave frequency versus $|\alpha - \beta|$ for different current velocity: k_x/k =1 and k_x/k =0.5.

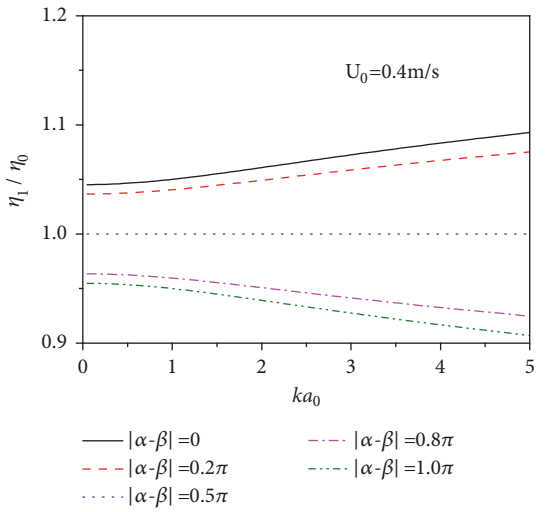

FIGURE 6: Effect of current on the wave run-up on the composite bucket foundation versus the ka_0 for different $|\alpha - \beta|$.

It should be noted that the wave run-up on the foundation under the wave-current is larger than that under wave when $|\alpha-\beta| < 0.5\pi$, whereas the wave-current interaction decreases the wave run-up on the foundation when $|\alpha - \beta| > 0.5\pi$. As shown in Figure 5, these results are consistent with the changes of the wave frequency. It also can be seen that the current has no influence on the wave run-up when $|\alpha - \beta| = 0.5\pi$, because the current has no effect on wave frequency. Consistent with the changes of the wave frequency, the wave run-up and the wave forces on the composite foundation become larger with the increase of current velocity when the relative angle is smaller than 90°. Figure 6 shows the ratio η_1/η_2 at $\theta = \pi$ on the composite bucket foundation against variable ka_0 for different $|\alpha - \beta|$ with U_0= 4m/s, where η_1 and η_2 denote the wave run-up under wave-current and wave. It can be seen that the effect of wave-current interaction on the short-crested wave run-up obviously increases with the increase of ka_0.

Figure 7 illustrates the variation of the total horizontal short-crested wave force on the composite bucket foundation versus the ka_0 for different $U_0$and $|\alpha - \beta|$ with k_x/k=0.5. In Figure 7, regardless of the values of current velocity, the wave force reaches a maximum value at low frequency and then decreases gradually. The total wave force obviously increases with increasing current velocity when the current incident angle parallels to the direction of the wave propagating, whereas it decreases with increasing current velocity when the current incident angle inverses to the direction of the wave propagating. Figure 8 illustrates the ratio F_1/F_2 against

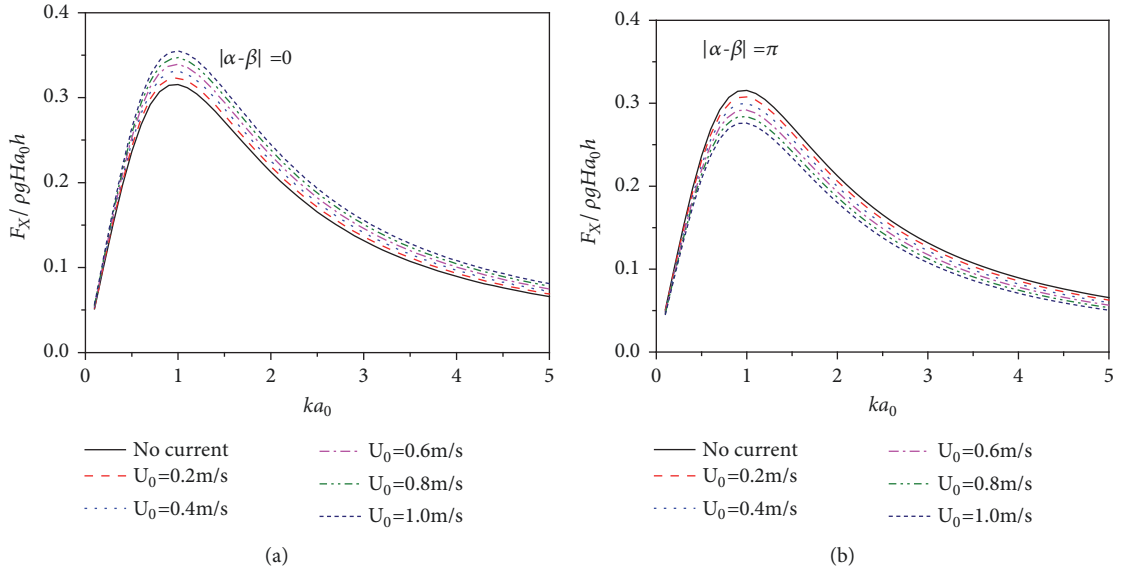

Figure 7: Variation of the total wave force on the composite bucket foundation versus the ka_0 for different current velocity with $k_x/k = 0.5$: (a) $|\alpha - \beta| = 0$ and (b) $|\alpha - \beta| = \pi$.

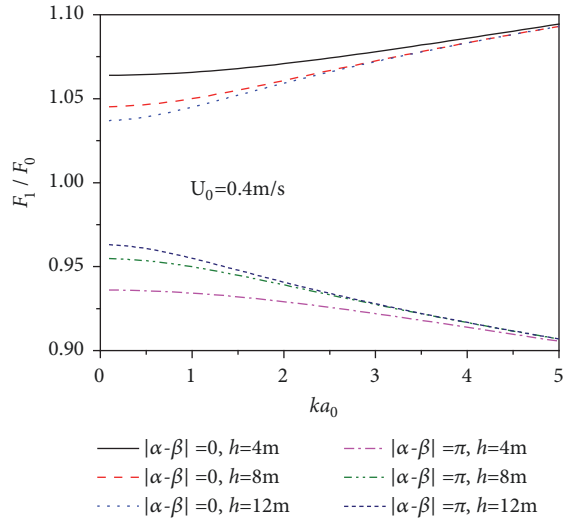

Figure 8: Effect of current on the total wave force on the composite bucket foundation versus the ka_0 for different $|\alpha - \beta|$.

variable ka_0 for different water depth with U_0= 4m/s, where F_1 and F_2 denote the total wave force under wave-current and wave. It can be seen that the effect of wave-current interaction on the wave force on the composite bucket foundation significantly decreases with the increase of water depth. The studies performed by Wang et al. (2018) indicate that the maximum wave force on the composite bucket foundation is achieved when the incident waves are the plane waves and it is conservative for the composite bucket foundation if the formula derived from the plane waves is used to estimate the wave force in a short-crested ocean. The results in the present study indicate that the maximum wave force on the composite bucket foundation is achieved when the current incident angle parallels to the direction of the wave propagating.

Figure 9 shows the variation of the inertia coefficient C_M and drag coefficient C_D on a circular cylinder versus the ka_0 for different conditions with $\alpha = \beta$. The conclusion can be drawn that the inertia and drag coefficients on a circular cylinder under wave are only relevant to the value of ka, whereas the inertia and drag coefficients on a circular cylinder under wave and current are still relevant to the radius of the cylinder, water depth, and current velocity. Figure 10 shows the variation of the inertia and drag coefficients at different location on the composite bucket foundation versus the ka_0 with U_0= 0m/s. It should be noted that the inertia and drag coefficients at different location on a circular cylinder is the same. However, the inertia and drag coefficients at different location on the composite bucket foundation is quite different, as shown in Figure 10. Figure 11 shows the variation of the inertia and drag coefficients on a circular cylinder versus the $|\alpha-\beta|$ with ka=1, a=2m, and h=8m. Figure 12 shows the variation of the inertia and drag coefficients at z=0.5h on the composite bucket foundation versus the $|\alpha - \beta|$ with ka_0=1 and h=8m. It can be seen from Figures 11 and 12 that the inertia and drag coefficients obviously increase with the increases of current velocity when $|\alpha - \beta| < 0.5\pi$, whereas the inertia and drag coefficients obviously decrease with the increases of current velocity.

5. Conclusions

A new analytical solution for the diffraction of short-crested waves with currents around a bottom-mounted composite bucket foundation was derived in this study. The wave run-up, the wave forces, and the inertia and drag coefficients are determined. It is obtained that current incident angle and current velocity have significant effects on the short-crested wave

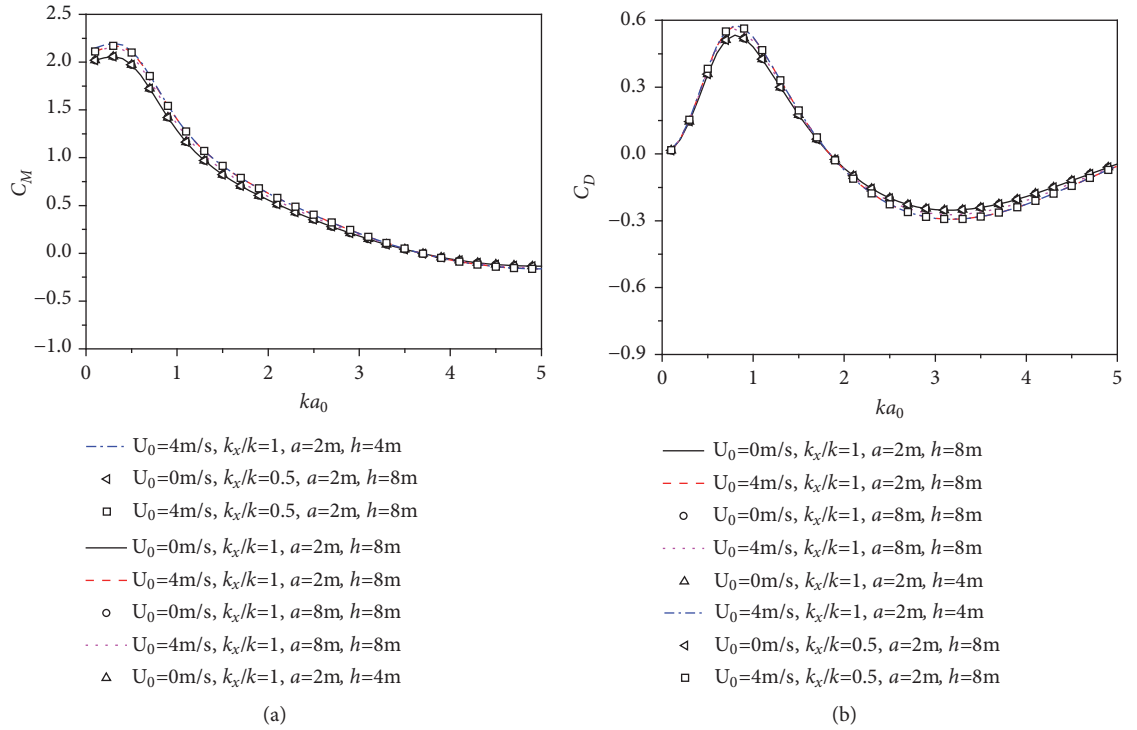

FIGURE 9: Variation of the inertia coefficient C_M and drag coefficient C_D on a circular cylinder versus the ka_0 for different conditions: (a) C_M and (b) C_D.

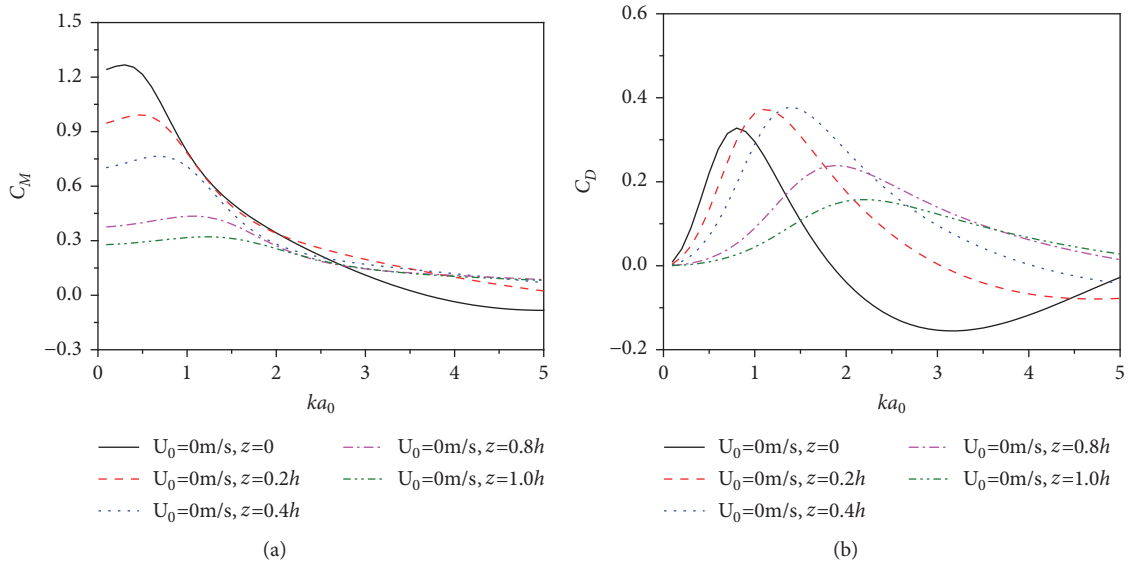

FIGURE 10: Variation of the inertia coefficient C_M and drag coefficient C_D at different location on the composite bucket foundation versus the ka_0: (a) C_M and (b) C_D.

run-up on the composite bucket foundation, which is mainly because the wave frequency of the short-crested wave system is significantly affected by current incident angle and current velocity. The maximum wave forces are achieved when the current incident angle parallels to the direction of the wave propagating. The effect of wave-current interaction on the short-crested wave obviously increases with the increase of the total wave number and obviously decreases the increase of the water depth. The inertia and drag coefficients obviously increase with the increases of current velocity when the relative angle is smaller than 90°, whereas these coefficients obviously decrease when the relative angle is larger than 90°.

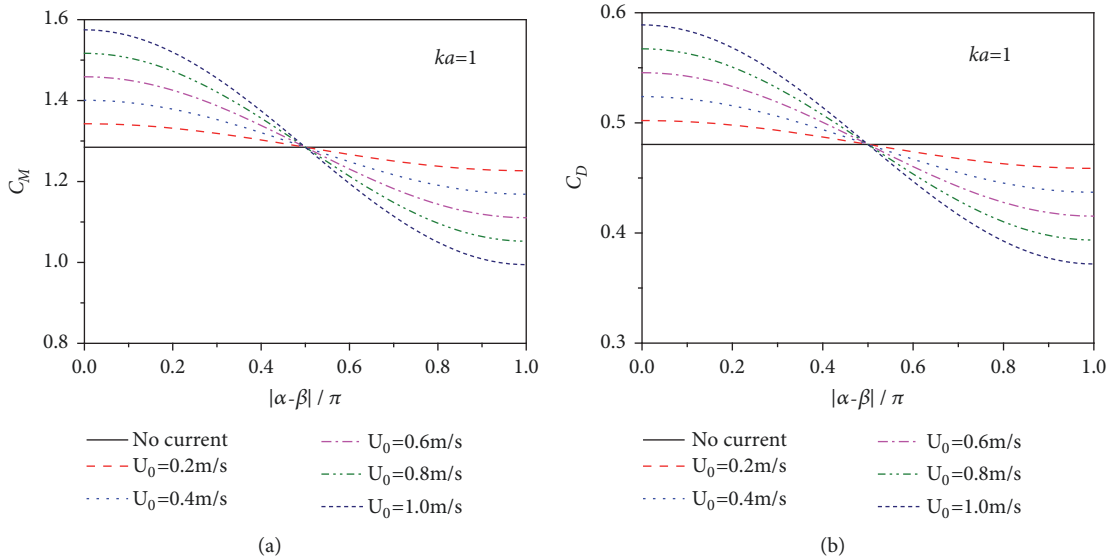

FIGURE 11: The inertia coefficient C_M and drag coefficient C_D on a circular cylinder versus $|\alpha - \beta|$ for different current velocity with ka_0=1: (a) C_M and (b) C_D.

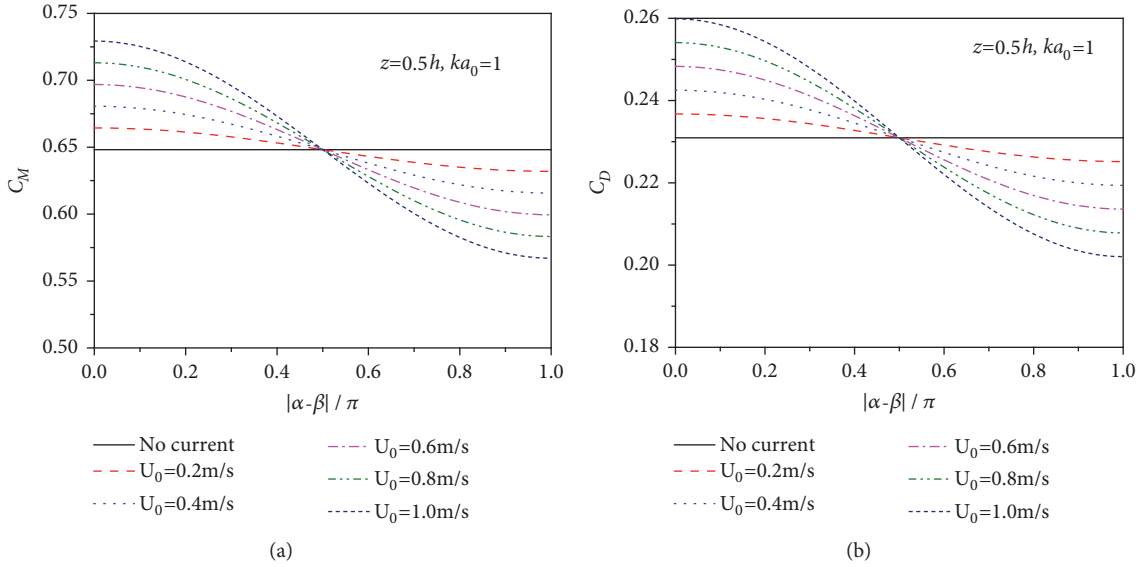

FIGURE 12: The inertia coefficient C_M and drag coefficient C_D at z=0.5h on the composite bucket foundation versus $|\alpha - \beta|$ for different current velocity with ka_0=1: (a) C_M and (b) C_D.

Data Availability

No data were used to support this study.

Conflicts of Interest

The authors declare that there are no conflicts of interest regarding the publication of this paper.

Acknowledgments

This research is jointly funded by the class General Financial Grant from the China Postdoctoral Science Foundation (2017M610901), the Foundation for Innovative Research Groups of the National Natural Science Foundation of China (51421005), and the National Natural Science Foundation of China (51722801 and 51878384).

References

[1] G. Failla and F. Arena, "New perspectives in offshore wind energy," *Philosophical Transactions of the Royal Society A: Mathematical, Physical & Engineering Sciences*, vol. 373, no. 2035, pp. 1–22, 2015.

[2] Y. Li and L. Duan, "Status of large scale wind turbine technology development abroad," *Applied Mathematics and Mechanics-English Edition*, vol. 37, no. S1, pp. S117–S124, 2016.

[3] B. W. Byrne and G. T. Houlsby, "Foundations for offshore wind turbines," *Philosophical Transactions of the Royal Society A: Mathematical, Physical & Engineering Sciences*, vol. 361, no. 1813, pp. 2909–2930, 2003.

[4] X. Y. Zheng, H. Li, W. Rong, and W. Li, "Joint earthquake and wave action on the monopile wind turbine foundation: An experimental study," *Marine Structures*, vol. 44, pp. 125–141, 2015.

[5] K. Wei, S. R. Arwade, A. T. Myers et al., "Toward performance-based evaluation for offshore wind turbine jacket support structures," *Journal of Renewable Energy*, vol. 97, pp. 709–721, 2016.

[6] L.-W. Zhang and X. Li, "Dynamic analysis of a 5-MW tripod offshore wind turbine by considering fluid–structure interaction," *China Ocean Engineering*, vol. 31, no. 5, pp. 559–566, 2017.

[7] E. Y. Choi, J. R. Cho, Y. U. Cho et al., "Numerical and experimental study on dynamic response of moored spar-type scale platform for floating offshore wind turbine," *Structural Engineering and Mechanics*, vol. 54, no. 5, pp. 909–922, 2015.

[8] Z. Da, Z. Xiliang, H. Jiankun, and C. Qimin, "Offshore wind energy development in China: Current status and future perspective," *Renewable & Sustainable Energy Reviews*, vol. 15, no. 9, pp. 4673–4684, 2011.

[9] J. Lian, L. Sun, J. Zhang, and H. Wang, "Bearing capacity and technical advantages of composite bucket foundation of offshore wind turbines," *Transactions of Tianjin University*, vol. 17, no. 2, pp. 132–137, 2011.

[10] J.-F. Zhang, X.-N. Zhang, and C. Yu, "Wave-induced seabed liquefaction around composite bucket foundations of offshore wind turbines during the sinking process," *Journal of Renewable and Sustainable Energy*, vol. 8, no. 2, Article ID 023307, 2016.

[11] P. Zhang, H. Ding, and C. Le, "Hydrodynamic motion of a large prestressed concrete bucket foundation for offshore wind turbines," *Journal of Renewable and Sustainable Energy*, vol. 5, no. 6, Article ID 063126, 2013.

[12] P. Zhang, K. Xiong, H. Ding, and C. Le, "Anti-liquefaction characteristics of composite bucket foundations for offshore wind turbines," *Journal of Renewable and Sustainable Energy*, vol. 6, no. 5, Article ID 053102, 2014.

[13] J. R. Morison, M. P. O'Brien, J. W. Johnson, and S. A. Schaaf, "The forces exerted by surface wave on piles," *Journal of Petroleum Technology*, vol. 189, pp. 149–154, 1950.

[14] R. C. MacCamy and R. A. Fuchs, "Wave forces on piles: a diffraction theory," Technical Memorandum No. 69, US Army Corps of Engineering, Beach Erosion Board, 1954.

[15] S. K. Chakrabatri and A. Tam, "Interaction of waves with large vertical cylinder," *Journal of Ship Research*, vol. 19, pp. 22–33, 1975.

[16] S. Neelamani, V. Sundar, and C. P. Vendhan, "Dynamic pressure distribution on a cylinder due to wave diffraction," *Ocean Engineering*, vol. 16, no. 4, pp. 343–353, 1989.

[17] P. Bettess and O. C. Zienkiewicz, "Diffraction and refraction of surface waves using finite and infinite elements," *International Journal for Numerical Methods in Engineering*, vol. 11, no. 8, pp. 1271–1290, 1977.

[18] T.-K. Tsay, W. Zhu, and P. L.-F. Liu, "A finite element model for wave refraction, diffraction, reflection and dissipation," *Applied Ocean Research*, vol. 11, no. 1, pp. 33–38, 1989.

[19] H. S. Chen and C. C. Mei, "Wave forces on a stationary platform of elliptical shape," *Journal of Ship Research*, vol. 17, no. 2, pp. 61–71, 1973.

[20] A. N. Williams, "Wave forces on an elliptic cylinder," *Journal of Waterway, Port, Coastal, and Ocean Engineering*, vol. 111, no. 2, pp. 433–439, 1985.

[21] F. P. Chau and R. Eatock Taylor, "Second-order wave diffraction by a vertical cylinder," *Journal of Fluid Mechanics*, vol. 240, pp. 571–599, 1992.

[22] B. Li, L. Cheng, A. J. Deeks, and M. Zhao, "A semi-analytical solution method for two-Helmholtz equation," *Applied Ocean Research*, vol. 28, no. 3, pp. 193–207, 2006.

[23] N. H. Kim, M. S. Park, and S. B. Yang, "Wave force analysis of the vertical circular cylinder by boundary element method," *KSCE Journal of Civil Engineering*, vol. 11, no. 1, pp. 31–35, 2007.

[24] H. Song, L. Tao, and S. Chakrabarti, "Modelling of water wave interaction with multiple cylinders of arbitrary shape," *Journal of Computational Physics*, vol. 229, no. 5, pp. 1498–1513, 2010.

[25] J. Liu, A. Guo, and H. Li, "Analytical solution for the linear wave diffraction by a uniform vertical cylinder with an arbitrary smooth cross-section," *Ocean Engineering*, vol. 126, pp. 163–175, 2016.

[26] S. Zhu, "Diffraction of short-crested waves around a circular cylinder," *Ocean Engineering*, vol. 20, no. 4, pp. 389–407, 1993.

[27] S. Zhu and G. Moule, "Numerical calculation of forces induced by short-crested waves on a vertical cylinder of arbitrary cross-section," *Ocean Engineering*, vol. 21, no. 7, pp. 645–662, 1994.

[28] S. Zhu and P. Satravaha, "Second-order wave diffraction forces on a vertical circular cylinder due to short-crested waves," *Ocean Engineering*, vol. 22, no. 2, pp. 135–189, 1995.

[29] L. Tao, H. Song, and S. Chakrabarti, "Scaled boundary FEM solution of short-crested wave diffraction by a vertical cylinder," *Computer Methods Applied Mechanics and Engineering*, vol. 197, no. 1-4, pp. 232–242, 2007.

[30] C. Chao Tung and N. E. Huang, "Influence of wave-current interactions on fluid force," *Ocean Engineering*, vol. 2, no. 5, pp. 207–218, 1973.

[31] R. K. Watanabe, *The Effect of Wave-Current Interactions on the Hydrodynamic Loading of Large Offshore Structures [PhD Thesis]*, Graduate College of Texas A&M University, 1982.

[32] Y. Jian, J. Zhan, and Q. Zhu, "Short crested wave-current forces around a large vertical circular cylinder," *European Journal of Mechanics - B/Fluids*, vol. 27, no. 3, pp. 346–360, 2008.

[33] J.-J. Lian, T.-S. Yu, and J.-F. Zhang, "Wave force on composite bucket foundation of an offshore wind turbine," *Journal of Hydrodynamics*, vol. 28, no. 1, pp. 33–42, 2016.

[34] P. Wang, M. Zhao, and X. Du, "Short-crested, cnoidal, and solitary wave forces on composite bucket foundation for an offshore wind turbine," *Journal of Renewable and Sustainable Energy*, vol. 10, Article ID 023305, 2018.

[35] R. A. Fuchs, "On the theory of short-crested oscillatory waves," in *Gravity Waves, National Bureau of Standards Circular No. 521*, pp. 187–200, Department of Commerce, USA, 1952.

[36] F. Arena and A. Romolo, "Random forces on a slender vertical cylinder given by high sea waves interacting with a current," *International Journal of Offshore and Polar Engineering*, vol. 15, no. 1, pp. 21–27, 2005.

[37] P. Boccotti, F. Arena, V. Fiamma, and A. Romolo, "Two small-scale field experiments on the effectiveness of Morison's equation," *Ocean Engineering*, vol. 57, pp. 141–149, 2013.

[38] C. C. Mei, *The Applied Dynamics of Ocean Surface Waves*, World Scientific, 1989.